

This document is confidential and is proprietary to the American Chemical Society and its authors. Do not copy or disclose without written permission. If you have received this item in error, notify the sender and delete all copies.

Noncatalytic bromination of icosahedral dicarboranes. The key role of anionic bromine clusters facilitating Br atom insertion into the B–H σ -bond

Journal:	<i>Inorganic Chemistry</i>
Manuscript ID	ic-2020-03392d.R1
Manuscript Type:	Article
Date Submitted by the Author:	29-Dec-2020
Complete List of Authors:	Shernyukov, Andrey; Novosibirskij institut organiceskoj himii imeni N N Vorozcova SO RAN, Laboratory of Magnetic Resonance Salnikov, George; Novosibirskij institut organiceskoj himii imeni N N Vorozcova SO RAN, Rudakov, Dmitry; N.N. Vorozhtsov Novosibirsk Institute of Organic Chemistry Of Siberian Branch of Russian Academy of Sciences, Genaev, Alexander; Vorozhtsov Novosibirsk Institute of Organic Chemistry SB RAS,

SCHOLARONE™
Manuscripts

Noncatalytic bromination of icosahedral dicarboranes. The key role of anionic bromine clusters facilitating Br atom insertion into the B–H σ -bond

Andrey V. Shernyukov, George E. Salnikov, Dmitry A. Rudakov and Alexander M. Genaev *

N.N. Vorozhtsov Institute of Organic Chemistry, Pr. Ak. Lavrentieva 9, Novosibirsk 630090, Russia. E-mail: genaev@nioch.nsc.ru.

Abstract

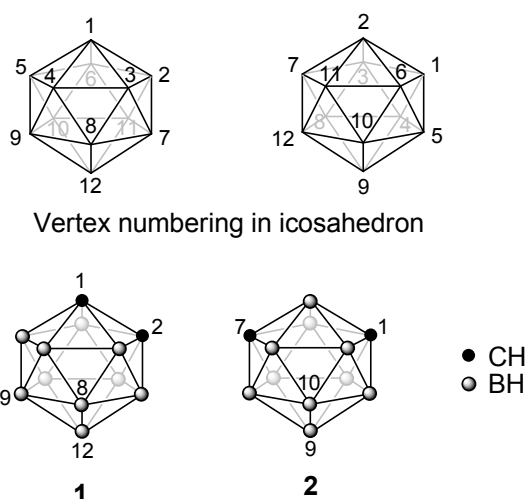
The mechanism of noncatalytic bromination of carboranes was studied experimentally and theoretically. We found that the reactions of *o*- and *m*-carboranes **1** and **2** with elemental bromine are first order in the substrate but unusually high (approximately 5th) order in bromine. Calculated energy barriers of these reactions decrease sharply as more bromine molecules are added to the quantum-chemical system. A considerable primary deuterium kinetic isotope effect for the bromination of **2** indicates that the rate-limiting stage is B–H bond breakage. According to quantum chemical reaction path calculations, the bond breakage proceeds after the intrusion of a bromine atom into the B–H σ -bond. The 9-Br and 9-OH substituents in carborane **1** strongly retard the bromination of the corresponding derivatives. The bromination mechanism of 9-OH-**1** is complex and includes neutral, deprotonated, and protonated forms of the carborane. High experimental kinetic reaction order in bromine, together with quantum chemical modeling, point to a specific mechanism of bromination facilitated by anionic bromine clusters which significantly stabilize the transition state.

Introduction

The reaction of electrophilic bromination is a textbook process and is of great importance both in synthetic and theoretical chemistry. It is well known that the reaction of nonactivated aromatic compounds, like benzene, with bromine requires the use of catalysts, Lewis acids. In our previous work, we showed that the bromination of benzene can be carried out under mild conditions and without a catalyst, provided that the concentration of bromine is sufficiently high.¹ A unique feature of this process is drastic acceleration of the reaction as the concentration of bromine increases. The reaction is enabled by clusters (associations of several molecules) of bromine that assemble during the reaction and stabilize the transition state (TS).² These bromine clusters are anion-like; therefore, a fundamental fact for their substantiation is the recent discovery of a series of cluster bromine anions Br_{2n-1}^- with $n > 3$ isolated in the crystalline state by Riedel's group.³

Earlier, the cluster mechanism of bromination has been investigated for traditional aromatic compounds: benzene and its derivatives. The present study is focused on carboranes, which possess a special type of aromaticity, 3D-aromaticity.⁴ The field of carborane science is growing accelerated in recent years.⁵ Just as ordinary aromatic compounds, carboranes participate in reactions of electrophilic substitution, which in this case affect boron atoms.⁶ Electrophilic bromination reactions of neutral C_2B_{10} -carboranes and nonactivated aromatic compounds with elemental bromine are usually carried out under similar conditions, in nonpolar aprotic solvents and in the presence of a Lewis acid as a catalyst. This similarity gives rise to the assumption of the applicability of an analogous bromination mechanism to carboranes. The aim of the present work is to verify this assumption for neutral icosahedral carboranes: *o*-carborane **1** and *m*-carborane **2** (Scheme 1). The choice of these compounds for this study is based on the fact that they are typical and most widely known representatives of carboranes and at the same time are relatively accessible.

Initially, the interest in the halogenation of carboranes was inspired by the similarity of their behavior in this reaction with the behavior of typical aromatic compounds. Practical interest in B-halogenated carboranes has remained limited because of the inertness of the halogen atom in terms of functionalization.⁷ Recently, however, techniques were developed that allow to create B–N⁸ and B–C bonds by cross-coupling according to the reactions of Kumada,^{9,10} Suzuki,^{11,12,13} and Heck^{14,15,16} (see also ref. 6). This approach opens up opportunities for the synthesis of new compounds with useful properties, including biologically active ones.^{9,17,18}



Scheme 1. Atom numbering in icosahedral carboranes

There are two kinds of arguments in favor of the cluster mechanism of bromination: experimental and theoretical.^{1,2} The experimental evidence—obtained when the reaction is carried out without a catalyst and at a high bromine concentration—is the high reaction order in bromine. For example, in the case of benzene, doubling of the bromine concentration leads to 30-fold acceleration of bromination, which corresponds to approximately the 5th order of the reaction with respect to bromine.¹ The theoretical argument supporting the participation of bromine clusters is a sharp decrease in the calculated bromination energy barrier as the number of bromine molecules in the quantum chemical system increases. Thus, for benzene bromination, the ratio of the reaction rates predicted by the Eyring equation from DFT energy barriers is 1:10⁶:10¹⁴:10¹⁷ for one, two, three, and four bromine molecules, respectively.

The arguments in favor of the participation of anionic bromine clusters in the bromination reaction suggest that the remaining part of the reacting system is cationic but do not give an insight into the specific mechanism of substitution of the boron-bonded hydrogen atom in the carborane cage by a bromine atom. Several years ago, it was stated¹⁹ that “Little is known with certainty about the substitution mechanisms on deltahedral boranes and carboranes, since no mechanistic studies seem to have been performed.” At the moment, from the results of calculations given in refs. 20 and 21, one can draw a conclusion that two alternative mechanisms are possible: H insertion into the Br–Br bond and Br insertion into the B–H bond. It is of interest to reveal a preference for one mechanism over the other.

Results and discussion

The bromination reaction was carried out in an NMR tube at 23 °C, and the concentration of carboranes was determined by the integration of ¹H and/or ¹¹B NMR spectra. Liquid bromine diluted with CCl₄ to a required concentration served as a solvent. In addition, each sample contained CD₂Cl₂ as a lock substance. CD₂Cl₂ (ε 8.9) is more polar than liquid Br₂ (ε = 3.1²²) and CCl₄ (ε = 2.2). It can noticeably increase the rate of bromination,¹ and therefore the concentration of CD₂Cl₂ (20 vol.%) was kept constant in all kinetic experiments. Because the kinetics were studied with a large excess of bromine (at least 20-fold), changes in its concentration during the reaction could be ignored. Under these conditions, the bromination of carboranes **1** and **2** was pseudo-unimolecular, but the reaction rate increased dramatically with increasing Br₂ concentration (Table 1, full experimental details can be found in Supporting Information [SI]). No difference was observed in either reaction rates or the composition of products, regardless of whether the experiments were conducted under light or in the dark. The experimental kinetics were evaluated by numerical integration of differential equation systems followed by nonlinear least-squares fitting of the relevant rate constants. The complete processing algorithm was implemented in the form of a SciLab²³ script.

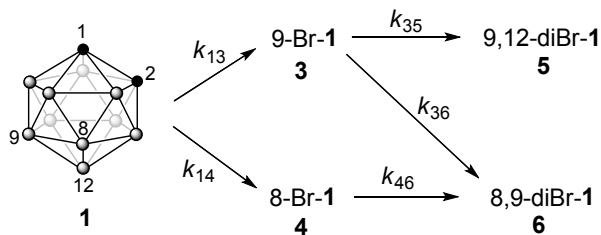
Bromination of *o*-carborane 1

Bromination rate constants of *o*-carborane **1** were determined by the integration of ¹H NMR signals of CH groups (SI, p. S41–S48). At a high bromine concentration (~80 vol.%), monobromination proceeds rapidly (95% completion in 10 min), giving 9- and 8-bromo-*o*-carboranes **3** and **4** in a ratio of 20:1 (SI, p. S7 and S8). With a decrease in the bromine concentration, the reaction slows down sharply (Table 1). The temperature decrease from 23 to –1 °C also results in a slowdown but not as much as one would expect according to the rule "20 degrees – by an order of magnitude." Such reduced sensitivity to temperature has also been reported regarding noncatalytic bromination of benzene.¹ This phenomenon may be regarded as a distinctive feature of the participation of bromine clusters, because their assembly during the formation of the reaction complex could induce a considerable entropy effect. After the first stage, bromination continues much more slowly and leads to dibrominated products. Note the much stronger deactivating influence of the bromine atom in *o*-carborane relative to that in benzene (a 165–407-fold vs. 8–13-fold retardation under the same conditions [1, SI, pp. S4, S9]). Apparently, this is because the Br substituent effects –I and +M for bromobenzene are mutually compensating, whereas for bromo-carborane, the activating +M effect is turned off. The products of double bromination of *o*-carborane **1** are 9,12- and 8,9-dibromo-*o*-carboranes **5** and **6** in a 4:1 ratio (SI, p. 10–24). The whole process is described by the kinetic system presented in Scheme 2. Kinetic curves of the second bromination step obtained by the integration of ¹¹B{¹H} NMR spectra are shown in Figure 1 (see also SI, p. S50), the fitted rate constants are as follows: $k_{13} = (417 \pm 30) \times 10^{-5}$, $k_{14} = (23 \pm 2) \times 10^{-5}$, $k_{35} = (0.867 \pm 0.04) \times 10^{-5}$, $k_{36} = (0.10 \pm 0.05) \times 10^{-5}$, and $k_{46} = (2.4 \pm 0.2) \times 10^{-5} \text{ s}^{-1}$.

Table 1. First-order rate constants k_1 of the bromination of carboranes

Carborane	Solvent, mL			Temperature	Concentration of Br ₂ , mol/L	$k_1 \times 10^{-5}, \text{ s}^{-1}$
	Br ₂	CCl ₄	CD ₂ Cl ₂			
1	0.15	0.25	0.1	23 °C	5.7	3.15
	0.2	0.2	0.1	23 °C	7.4	19.8
	0.2	0.2	0.1	–1 °C	7.6	3.16
	0.3	0.1	0.1	23 °C	11.1	100.1
	0.4	–	0.1	23 °C	14.8	440
	0.4	–	0.1	–1 °C	15.1	133
2	0.2	0.2	0.1	23 °C	7.6	0.299
	0.3	0.1	0.1	23 °C	11.5	2.45
	0.4	–	0.1	23 °C	15.3	12.3
Br-1^a	0.15	0.25	0.1	23 °C	5.7	0.019
	0.2	0.2	0.1	23 °C	7.4	0.0744
	0.3	0.1	0.1	23 °C	11.1	0.302
	0.4	–	0.1	23 °C	14.8	1.08

^aThe ¹H NMR signals of the CH groups of carboranes **3** and **4** are completely overlapped; their bromination rate constants refer to a mixture of **3** and **4** designated as **Br-1** (SI, p. S49)



Scheme 2. Kinetic system for bromination of carborane **1**

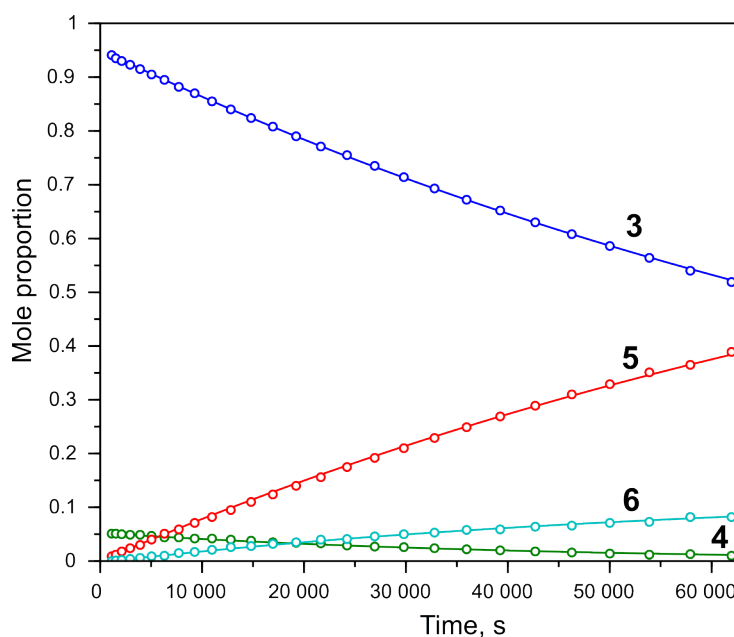
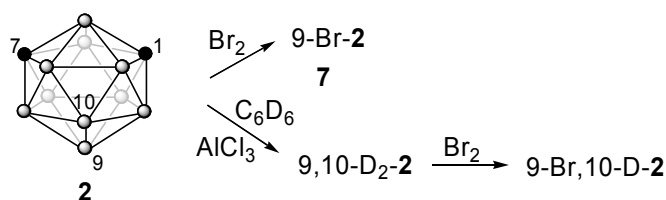


Figure 1. Bromination kinetics of the mixture of mono-Br-carboranes **Br-1** ($[\text{Br}_2] = 14.8 \text{ mol/L}$, 23°C). Experimental data points are denoted by circles, and fitted curves by solid lines

Comparisons of rate constants k_{13} vs. k_{14} and k_{35} vs. k_{36} revealed that the bromination at position 9 (12) is 18-fold faster than that at position 8 (10), taking into account the molecular symmetry. This regioselectivity is in line with the general tendency for carboranes, namely, that boron atoms that are remotest from carbon atoms are most active in electrophilic processes.⁶ On the other hand, the difference in rate constants k_{35} vs. k_{46} is mainly due to a statistical factor (k_{46} must be divided by two). Thus, the deactivating influence on the bromination rate at adjacent position 12 for the 9-Br substituent is only slightly stronger than that for the 8-Br substituent.

Bromination of *m*-carborane **2** and a kinetic isotope effect (KIE)

Noncatalytic bromination of *m*-carborane **2** proceeds selectively. The only reaction product is 9-bromo-*m*-carborane **7** (Scheme 3; SI, p. S38–S40); no further bromination takes place. The bromination rate constants (Table 1) were determined by the integration of B9,10 signals in ^{11}B $\{^1\text{H}\}$ NMR spectra (SI, p. S51–S54). Depending on the bromine concentration, the rate for *m*-carborane **2** is 36–66-fold lower than that for *o*-carborane **1** under the same conditions (Table 1). Note that *m*-carborane **2** is only 7-fold less active than *o*-carborane **1** when the reaction is carried out in the presence of a catalyst.²⁴



Scheme 3. Bromination of carboranes **2** and **2-d₂**

KIEs are widely used to elucidate mechanisms of electrophilic substitution.²⁵ If the rate-limiting step is the B–H bond cleavage, then a large primary deuterium isotope effect should be expected. The synthesis of deuterated carborane 9,10-D₂-**2** (SI, p. 56) was conducted based on the data from ref. 26. Here, *m*-carborane **2** was chosen because its bromination proceeds more cleanly as opposed to *o*-carborane **1**. An additional convenience is that the signals of boron nuclei at B9,10 reaction centers in **2** are free of overlaps with other signals, thereby facilitating data processing. Nevertheless, KIE measurements appeared to be impeded by several experimental difficulties.

Firstly, deuterated carborane yields only the sum of primary and α -secondary KIEs not the pure primary KIE. Fortunately, the α -secondary KIE can be ignored because secondary KIEs tend to be much smaller than primary ones (see calculation data below).

Secondly, the most reliable method usually applied for determining a KIE is a competitive reaction with a mixture of deuterated and nondeuterated predecessors. Nonetheless, during bromination, HBr (or DBr) forms, which is a strong acid in nonaqueous low-nucleophilic media. In the presence of elemental bromine playing the role of a Lewis acid,²⁷ HBr acidity increases further, approaching that of a superacid. This side process can induce rapid averaging of the H/D distribution in both substrates and products, making the evaluation of a KIE impossible.² Indeed, in an experiment in a superacid (deuterated trifluoromethanesulfonic acid), the H/D exchange at positions 9 and 10 of *m*-carborane **2** reached 50% completion in less than 1 h (SI, p. S55). Fortunately, an experiment on *m*-carborane bromination—in the presence of an excess of DBr generated *in situ* in more rapid parallel bromination of explicitly added C₆D₆—showed that no deuterium entered the carborane molecule (SI, p. S57). Therefore, the KIE distortion due to H/D exchange in *m*-carborane can be excluded.

Finally, the determination of bromination rate constants for substrates **2** and 9,10-D₂-**2** was performed by three methods independently. In the first case, an equimolar mixture of substrates was brominated, and ¹¹B NMR spectra were integrated through signal deconvolution (Fig. 2, SI p. S60 and S61). In the second case, also related to the bromination of a mixture of substrates, INEPT ¹¹B{¹H} spectra were integrated. Only B–H signals appeared in such spectra, but B–D and B–Br signals did not (SI, p. S59). In the third case, the substrates were brominated in separate experiments with conventional integration of ¹¹B{¹H} spectra (SI, p. S53 and S58). The obtained KIE values were 2.0, 2.7, and 2.3, respectively.

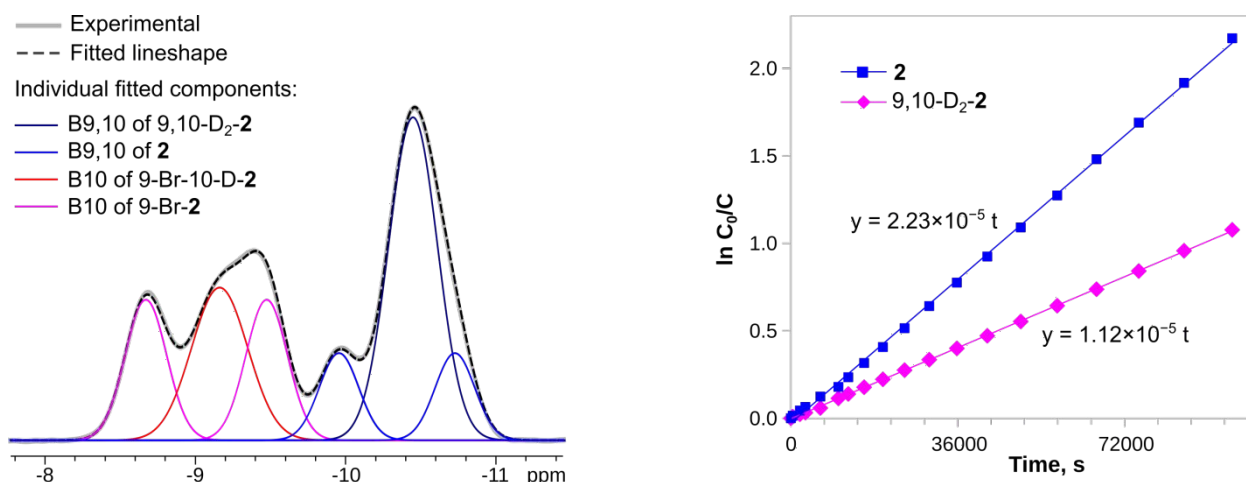


Figure 2. Bromination of **2** + 9,10-D₂-**2** ([Br₂] 11.3 mol/L, 23 °C). Left: A representative ¹¹B NMR spectrum of a reaction mixture (the B9,10 region, after 18 h) and deconvolution of the signals (MagicPlot software,²⁸ components of B–H doublets are constrained to equality); right: kinetic plots “ln(C₀/C) vs. time.”

We believe that the results of the first method should be regarded as the most reliable. The results of the second method can be distorted due to some influence of J-modulation on INEPT spectra, whereas the data from the third method may be affected by slightly nonidentical conditions inevitable for individual experiments. Anyway, the KIE after noncatalytic bromination of *m*-carborane is significantly different from unity. Therefore, there is no doubt that the rate-limiting stage of the reaction is B–H bond breakage.

The reaction order in bromine

An important attribute of the participation of bromine clusters is extremely high order of the reaction with respect to bromine. The reaction order was determined by a differential method²⁹ using kinetic eqs. (1) and (2) relating pseudo-first-order kinetics at different bromine concentrations to a formal reaction of the $n + 1$ order, respectively.

$$-d[\text{Ar}]/dt = k_1 [\text{Ar}] \quad (1)$$

$$-d[\text{Ar}]/dt = k_{n+1} [\text{Ar}] [\text{Br}_2]^n \quad (2)$$

$$\log k_1 = n \log [\text{Br}_2] + \log k_{n+1} \quad (3)$$

After plugging the kinetic data (Table 1) into eq. (3), the reaction order with respect to bromine was determined (Table 2, Figure 3). For comparison, the data on noncatalytic bromination of benzene¹ are also presented; benzene occupies an intermediate position between *o*- and *m*-carboranes **1** and **2** in terms of reactivity.

Table 2. The reaction order in bromine (*n*) and $\log k_{n+1}$ for the bromination reactions at 23 °C.

Substrate	<i>n</i>	$\log k_{n+1}$
1	5.0±0.4	-8.2±0.4
1 ^a	5.3	-9.2
2	5.3±0.1	-10.3±0.1
Br- 1	4.1±0.2	-9.8±0.2
C ₆ H ₆ ¹	4.8±0.1	-9.2±0.1

^a At -1 °C

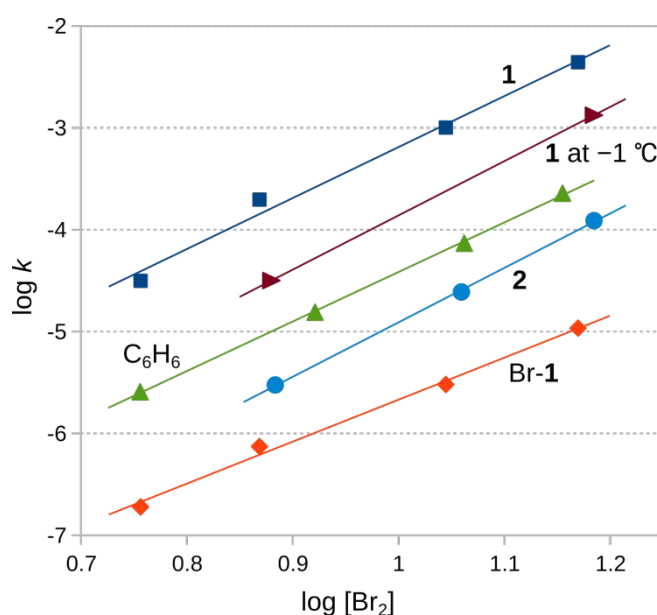


Figure 3. Determination of the reaction order in bromine. Order *n* is the tangent of the slope of the fitted linear functions.

At a bromine concentration of 1 mol/L, the k_{n+1} constant (Table 2) coincides with the k_1 constant and allows to estimate the rate of the bromination reaction at this concentration. This rate is extremely low (for example, $t_{1/2}$ was found to be 3 years for *o*-carborane **1** and is 35 years for benzene). Therefore, in the case of dilute bromine solutions, we can say that the bromination is virtually absent in the absence of a catalyst. This conclusion is consistent with the generally accepted notion of the inertness of neutral carboranes⁶ and nonactivated aromatic compounds [1, SI, p. S2] in noncatalytic bromination reactions. Our data give reason to clarify this thesis being applicable only to reactions in solutions with a relatively low concentration of bromine, which are commonly used in synthetic procedures.

The bromination of hydroxycarborane **8**

It was demonstrated above that the effects of the bromine atom on bromination rates of 9-Br-*o*-carborane **3** and bromobenzene are the same qualitatively but different quantitatively: the deactivating

impact of bromine in the carborane is more pronounced. In contrast to the Br substituent, the effects of the OH group differ qualitatively: phenol is much more active than benzene, whereas carborane **8** is less active than *o*-carborane **1**.³⁰

We compared bromination rates between *o*-carborane **1** and its hydroxy derivative **8** under the same conditions. The reaction was monitored by means of ¹H and ¹¹B{¹H} NMR spectra, with integration of the CH and B12 signals, respectively (SI, p. S62–S65). Unlike *o*-carborane **1** undergoing a first-order reaction with respect to the substrate, in the case of **8**, there is a strong deviation from monomolecularity (Fig. 4a). At the beginning of the reaction, compound **8** is brominated ~5-fold more slowly than *o*-carborane **1** is (Fig. 4b). Later, the reaction rate decreases even more, almost 100-fold as compared to the initial one. As a product of the bromination of **8**, mainly 9-hydroxy-12-bromo-*o*-carborane **9** forms (SI, p. S32–S34).

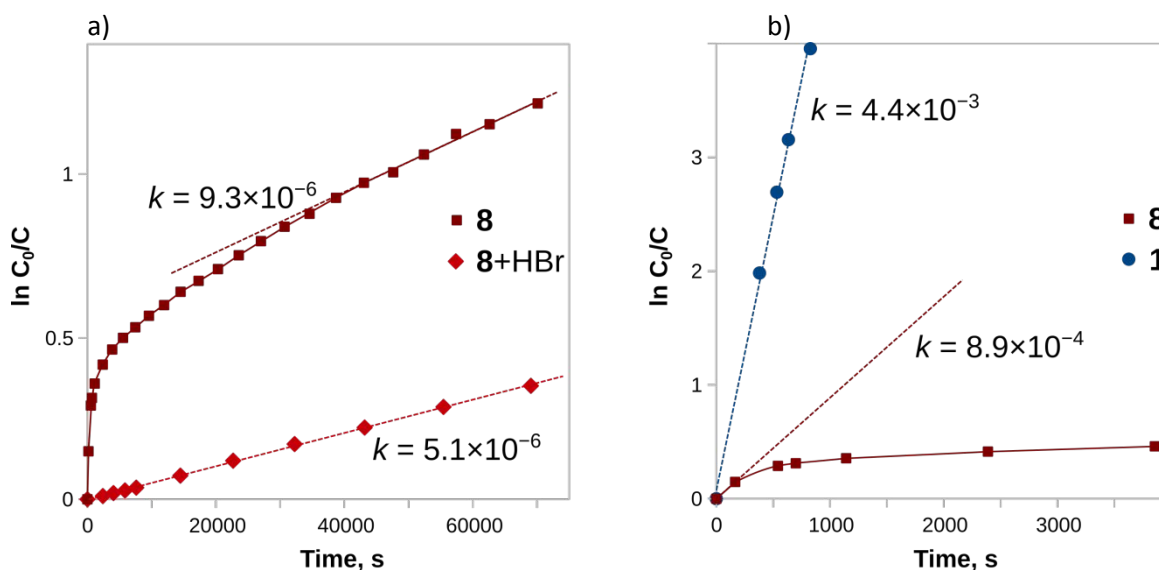
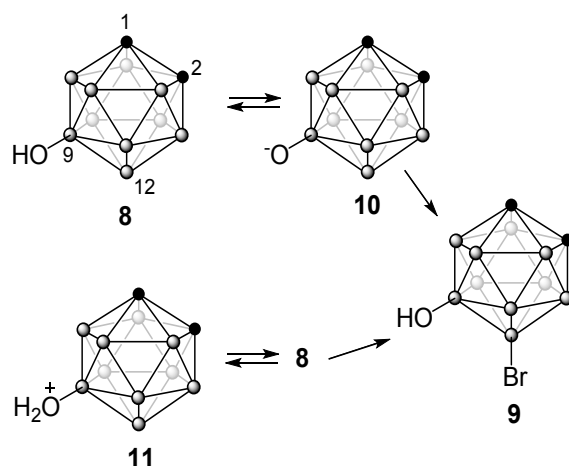


Figure 4. Bromination kinetics of **8** ($[\text{Br}_2] = 15 \text{ mol/L}$, 23°C ; kinetic plots “ $\ln(C_0/C)$ vs. time”)

The nonlinearity of the kinetic curve can occur due to two additional processes (Scheme 4). One of bromination products is HBr. Being a strong acid in the liquid-bromine medium, it is capable of partially protonating the OH group of carborane **8** giving oxonium cation **11**. Oxonium derivatives of polyhedral boron hydrides are well known.³¹ The fact of protonation is evidenced by the NMR data: the B9 signal of **8** is shifted to a high field (SI, p. S63)³² in the reaction course, and the ¹H NMR signal of the OH group (SI, p. S62) is shifted to a low field, toward R-OH_2^+ .³³ Protonated substrate **11** is apparently less active in electrophilic bromination. Indeed, the dependence of the reaction rate on HBr concentration is proved by an explicit experiment. An excess of HBr generated *in situ* from C_6H_6 decreases the rate of bromination of carborane **8**, and the kinetic curve becomes linear with a slight curvature appearing only when the reaction is deep (Fig. 4a; SI, p. S66). Being responsible for the decrease in the bromination rate constant at a later stage of the reaction, carborane **8** protonation cannot explain the sharp rate decrease at the initial stage, when the HBr concentration and, accordingly, the proportion of the protonated form is small. On the other hand, hydroxy carboranes, including **8**, are known to also have acidic properties.³⁴ It can be assumed that at the initial stage, deprotonated form **10**, not carborane **8** itself, is brominated. This deprotonated form is much more reactive, but its equilibrium contribution is low, and even the small amount of HBr formed at the very beginning of the reaction is sufficient to neutralize it. This mechanism is consistent with a sharp slowdown of the bromination at the initial stage.

A decrease in bromine concentration from 15 to 11.5 mol/L causes retardation of carborane **8** bromination (SI, p. S65). In this case, the kinetic-curve nonlinearity becomes less pronounced. The ratio of rate constants at the initial stage is 4.9, which corresponds to a sixth-order reaction with respect to bromine; at a later stage, the reaction order decreases.



Scheme 4. Bromination of carborane **8**

Quantum-chemical calculations

In addition to the evidence of the high experimental kinetic reaction order in bromine, the cluster mechanism of bromination can be confirmed theoretically by a sharp decrease in the reaction's energy barrier as the number of bromine molecules in a quantum-chemical system increases. To test such hypothesis, it is necessary to locate TSs of bromination reactions for systems carborane- Br_{2n} and to compare their energies at different values of n . The systems under consideration are conformationally nonrigid and have many possible stationary points on the potential-energy surface. Therefore, a fast DFT code implemented in the PRIRODA software³⁵ and employing a PBE functional³⁶ with full-electron basis $\Lambda 01$ ³⁷ similar to the cc-pVDZ basis set was chosen for our calculations.

Geometric parameters of the located TSs for the $1 + n\text{Br}_2$ reaction ($n = 1$ to 5) with lowest energies are given in Fig. 5 (see also SI, p. 69–76). For carborane **2**, the structures are similar (SI, p. 79–84). It is noteworthy that all structures, except for **1-Br₂**, are ion pairs with Br_{2n-1}^- clusters as anionic parts. Similar clustered bromine anions are known to form TSs during noncatalytic bromination of aromatic compounds.^{1,2} In contrast to those, in the case of carboranes, bromine clusters tend to wrap the carborane cage, not the reaction center. For example, TS **1-Br₆** in Fig. 6a is 7.6 kcal/mol less favorable than the TS in Fig. 5c. Small anionic clusters Br_3^- in **1-Br₄** and Br_5^- in **1-Br₆** are linear and V-shaped, respectively, just as the corresponding anions in widely studied polybromide salts.³ Nonetheless, larger clusters Br_7^- in **1-Br₈** and Br_9^- in **1-Br₁₀** with chain structure devoid of side branches become more favorable than the pyramidal and tetrahedral shapes^{3,38} characteristic for polybromide salts. For instance, TS **1-Br₈** in Fig. 6b is 6.5 kcal/mol higher in energy than the TS in Fig. 5d. An analogous preference for chained TS geometry with an increase in the volume of the reaction center wrapped by a cluster was noted in ref. 2. In the case of carboranes, the larger volume of the entire carborane backbone obviously plays a role. A characteristic feature of TSs with the lowest energies is the placement of the Br_{2n-1}^- ion on the opposite side of the eliminated hydrogen atom.

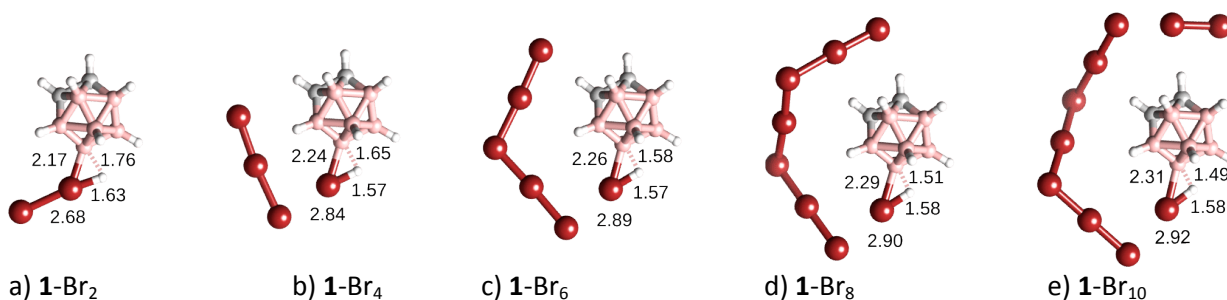


Figure 5. DFT/PBE/ $\Lambda 01$ TSs of reaction **1** + $n\text{Br}_2$ ($n = 1$ to 5). Numbers are interatomic distances (Å) in the reaction centers.

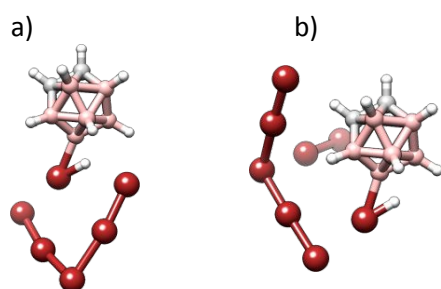


Figure 6. Alternative TSs for **1-Br₆** (a) and **1-Br₈** (b)

Inspection of intrinsic reaction coordinate (IRC) paths for the located TSs showed that the prereaction complex in all cases consists of individual bromine molecules weakly bound to the carborane, whereas the product is an unstable intermediate corresponding to the bromocarborane protonated at the bromine atom (Fig. 7). We did not follow further fate of these intermediates, but there is no doubt that they can be easily broken down into weakly bound molecular bromocarborane, HBr, and (n-1)Br₂, which are ~30 kcal/mol stabler than the initial system. The instability of such intermediates can be confirmed by data from ref. 20, according to which a similar adduct for the **1-Br₄** system was converted to products with a barrier of only 1.2 kcal/mol.

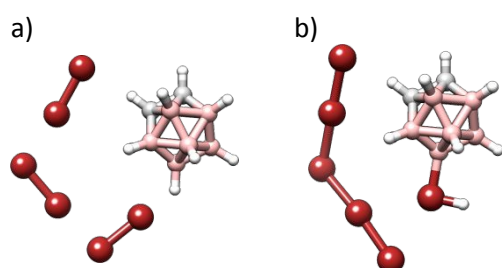


Figure 7. Pre- (a) and post- (b) reaction complexes for TS **1-Br₆** from Fig. 5

Usually, the energy difference between the TS and the prereaction complex resulting from an IRC is considered a reaction barrier. Our model is complicated by the fact that in the case of a supramolecular substrate with several weakly bound bromine molecules, an IRC descent yields only one of a variety of associations having significantly different energy levels, not necessarily the most stable one. For the analogous C₆H₆+3Br₂ system, the energies of various prereaction complexes are distributed within 12 kcal/mol.³⁹ To avoid uncertainty, the total energy of noninteracting substrate and bromine molecules was designated as the zero energy level. This approach at least guarantees the independence of the reaction barrier from the energy of a given prereaction complex, but it turned out that the total electron–nuclear DFT energies of TSs with three or more bromine molecules fall below the zero level. A reasonable arrangement of energy levels was obtained by adding thermodynamic corrections (Table 3).

Table 3. Energy E_{DFT/PBE/Λ01}+G₂₉₈ (kcal/mol) of the most favorable TSs for the reactions of carboranes **1** and **2** with n Br₂ (n = 1 to 5) relative to the total energy of noninteracting molecules.^a For *m*-carborane **2**, the calculated values of the KIE for **2** vs. 9,10-D₂-**2** are given too.

Reaction	Energy	Reaction	Energy	KIE
1 + Br ₂	35.9	2 + Br ₂	39.9	1.8
1 + 2Br ₂	28.0	2 + 2Br ₂	31.8	1.6
1 + 3Br ₂	19.9	2 + 3Br ₂	25.8	1.5 ^b
1 + 4Br ₂	18.7	2 + 4Br ₂	24.7	1.5
1 + 5Br ₂	18.3	2 + 5Br ₂	26.3	1.4

^a The sum of E_{DFT/PBE/Λ01}+G₂₉₈ energies of noninteracting molecules of carborane-Br, HBr, and (n-1)Br₂ is -32.5 kcal/mol for **1** and -31.0 kcal/mol for **2**. ^b The α-secondary KIE for **2** vs. 10-D-**2** is 0.97

The case of n = 1 is a model of low bromine concentration where the formation of clusters is unlikely. Noncatalytic bromination of carboranes **1** and **2** is known to not proceed under these

conditions,⁶ in line with very high predicted energy barriers. Based on quantum chemical calculations, the conclusion about high reaction barriers of noncatalytic electrophilic chlorination and bromination of carboranes has also been made elsewhere.^{20,21} With increasing n , the energy barriers decrease, and at $n > 2$, can be overcome at ambient temperature. At the same number of bromine molecules in the quantum-chemical system, the bromination barrier of *o*-carborane **1** is lower than that of *m*-carborane **2**. This notion is in agreement with higher inertness of the latter in the bromination reaction.

Experimental kinetic isotope effects can be used to validate computed TS models.⁴⁰ If the rate-limiting step is B–H bond cleavage, then a large primary H/D isotope effect can be expected. The DFT/PBE/Λ01 calculation for reactions 9,10-D₂-**2** + $n\text{Br}_2$ (Table 3) gave KIEs that differ from the experimental value downward. Examination of the potential energy surface of the **2**-Br₆ system near the TS showed that the B–H bond in the TS is only beginning to break (Fig. 8). It is possible that a slight shift of the TS location toward the reaction products increases the KIE thereby bringing it closer to the experimental value.

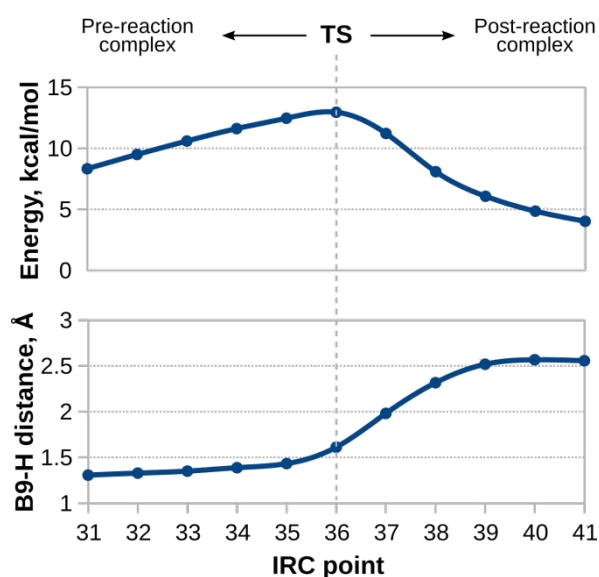


Figure 8. $E_{\text{DFT/PBE}/\Lambda 01}$ relative to the prereaction complex on the IRC around the **2**-Br₆ TS as well as the corresponding B9–H bond lengths.

An extreme amount of calculations required to search for TSs and to compute the IRC was performed in the PRIRODA software. This program is fast but supports calculations in a gas phase only and does not provide DFT-D3 corrections. The PBE functional used takes into account dispersion interactions but not fully.⁴¹ To refine the KIE, the **2**-Br₆ TS was reoptimized with the GAMESS-US software⁴² by the DFT/PBE/cc-pVDZ method, taking into consideration the PCM solvation model⁴³ and Grimme's D3 dispersion corrections.⁴⁴ For PCM, solvent radius 2.25 Å obtained from the van der Waals volume of the Br₂ molecule and experimental dielectric constant 3.1 of liquid bromine²² were used. Note that the geometry of the TS optimized by this method retained all the features described above for the gas phase structure. The KIE calculated with the solvation and dispersion corrections is 2.2, in good agreement with the experimental values (2.0–2.7).

Mechanistic insights

Noncatalytic bromination reactions of carboranes and of the simplest aromatic compound, benzene, share a number of similarities. In terms of reactivity, benzene occupies an intermediate position between *o*- and *m*-carboranes **1** and **2** (Fig. 3). It is close to carboranes in the reaction order (1st in the substrate and ~5th in bromine) and in the reduced sensitivity of the bromination rate to temperature. Nonetheless, despite numerous similar aspects the reaction mechanisms cannot be identical. It has been reported¹ that the TS structure during benzene bromination resembles the Weyland intermediate (Fig. 9), whereas for carboranes, such a structure is impossible.¹⁹ We believe that

all the similar features of the two reactions are determined by the ability of bromine to form clusters of the same type, and not related to structural peculiarities in the reaction centers of substrates.

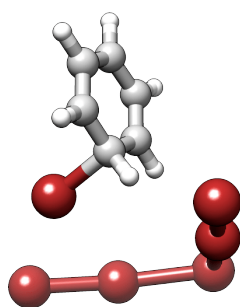


Figure 9. The TS of S_EAr concerted substitution for the $C_6H_6-Br_6$ system (B3LYP+D3/6-311++G(2d,2p)/SCRF=benzene)⁴⁵

The literature contains contradictory data on the detailed mechanism of electrophilic substitution at the boron atom in carboranes.

In an early work,⁴⁶ two mechanisms were considered: (a) the insertion of an electrophilic particle into the B–H bond with subsequent detachment of a proton and (b) the addition of the electrophilic particle to the electron-rich B–B bond followed by the abstraction of a proton and localization of the electrophile on one of B atoms. Note that for halogenation reactions, quantum chemical calculations do not confirm mechanism (b): neither in this work nor in those cited below, a TS was found in which a halogen atom forms a coordination bond with two boron atoms.

Possible mechanisms of electrophilic substitution for common aromatic compounds and carboranes were compared in ref. 19. For carboranes, along with the mechanism of type (a) considered above, those authors propose mechanism (c) involving the transfer of an electron from the carborane backbone to the electrophile. In the case of electroneutral carboranes **1** and **2**, the proposed mechanism implies a stage of dissociation of the carborane radical cation into the carborane cation and H^\bullet . According to calculations, this stage is strongly endothermic (by more than 40 kcal/mol), and therefore mechanism (c) seems unlikely in this context.

In a theoretical study,²¹ mechanism (d) was proposed, which consists (in relation to the bromination reaction) of the insertion of a hydrogen atom bound to the boron atom of the carborane backbone into the Br–Br bond (Fig. 10). Fig. 10 also shows a hidden intermediate⁴⁷ that lies on the IRC between the TS and products and allows to visually trace the reaction path.

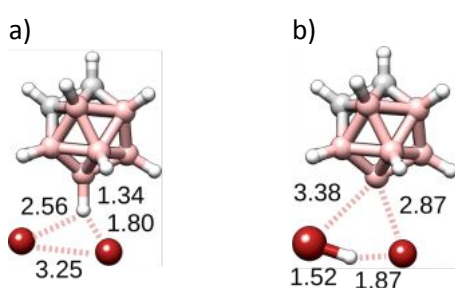
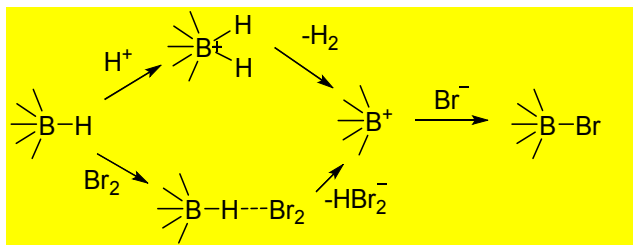


Figure 10. The TS a) and the hidden intermediate b) of the **1**+Br₂ reaction according to mechanism (d). The numbers are interatomic distances (Å) in the reaction centers.

In a recent study²⁰ on the bromination mechanism of *o*-carborane **1** and on the establishment of gas phase structure of reaction product **3**, reaction paths of **1** with one and two bromine molecules were calculated. For the **1**-Br₄ system, the TS of the limiting stage reported is very similar to that documented by us (Fig. 5b) and corresponds to a mechanism of type (a). For the **1**-Br₂ system, those authors propose a TS depicted in Fig. 10a corresponding to mechanism (d). According to our calculations, such a TS is 22 kcal/mol higher in energy than that for the insertion of a Br atom into the B–H bond (Fig. 5a). The same energy difference is involved in bromination at position 9 of *m*-carborane **2**. The increased energy barrier renders bromination mechanism (d) less likely.

The substitution reactions of cage boron hydrides, especially anionic ones, often follow the electrophile-induced nucleophilic substitution (EINS) mechanism.^{31,48,49} This mechanism implies a hydride ion abstraction followed by attack of a donor molecule (Scheme 5). Typical acceptors for hydrides in B–H moieties are Lewis acids, including $\text{BF}_3 \cdot \text{OEt}_2$, AlCl_3 , and H^+ .⁵⁰ The Brønsted acid proton is the most commonly used electrophile in EINS reactions.⁴⁹ In this case, the mechanism is called acid-assisted nucleophilic substitution (AANS).³¹



Scheme 5. AANS and EINS mechanisms

We believe that in our case the AANS mechanism can be rendered out based on experimental data. The initial reaction mixture (carborane + $\text{Br}_2 + \text{CD}_2\text{Cl}_2$) contains no acid, and nevertheless the reaction starts successfully. Later, a strong Brønsted acid (HBr) is formed, but it does not influence the reaction rate at all (it even inhibits the reaction in the special case of carborane **8**). The EINS mechanism with Br_2 playing the role of a Lewis acid may be considered. However, for neutral dicarboranes in liquid bromine such a mechanism is unlikely: the B–H moiety does not have a pronounced hydride character, and Br_2 is not a strong Lewis acid, either. Quantum chemical modeling predicts a concerted mechanism of carborane bromination. Bromine clusters Br_{2n-1}^- , independently on the number of Br_2 molecules involved, always tend to coordinate the carborane cage and not the hydrogen atom being eliminated (Fig. 5).

Thus, quantum chemical calculation results allow us to conclude that noncatalytic bromination of *o*- and *m*-carboranes with elemental bromine proceeds through the insertion of a bromine atom into the B–H σ -bond (mechanism (a)). An additional argument in favor of this mechanism is the agreement between the calculated and experimental KIE values.

Conclusions

From the results of the study, the following conclusions can be drawn:

- Reactions of noncatalytic bromination of *o*- and *m*-carboranes **1** and **2** with elemental bromine are first order in the substrate and high (approximately 5th) order in bromine.
- Theoretical energy barriers for the bromination drop sharply as more Br_2 molecules are added to the quantum chemical system. In a recent work,²⁰ a decrease in the barrier between systems **1**- Br_2 and **1**- Br_4 was reported, but systems with a larger number of Br_2 molecules were not considered.
- Conclusions i and ii taken together indicate the cluster mechanism of bromination in which the TS is stabilized by anionic bromine clusters Br_{2n-1}^- .
- The primary deuterium kinetic isotope effect for the bromination of carborane **2** with a value above 2.0 means that the rate-limiting stage of the reaction is B–H bond cleavage. Quantum chemical modeling suggests that the B–H bond breakage occurs after the intrusion of a bromine atom into this bond.
- Bromination of *o*-carborane **1** at position 9 (12) proceeds 18-fold faster than that at position 8 (10). The 9-Br atom strongly deactivates the carborane molecule in relation to the introduction of the second bromine atom, ~20-fold more strongly than in the case of benzene.
- The hydroxy group at position 9 of carborane **8** has a strong deactivating influence on adjacent position 12, where the bromination takes place. The reaction mechanism of the bromination of hydroxy carborane **8** is complicated. In contrast to carboranes **1** and **2**, the reaction is not first order in the substrate, and the reaction rate depends on HBr concentration. Apparently, both the deprotonated and protonated forms of carborane **8** participate in the reaction at different stages.
- The strong deactivating impact of the Br and OH substituents in carborane is explained by the absence of an activating mesomeric effect requiring a conjugated π -system.

We believe that the most intriguing feature of noncatalytic bromination is the high kinetic order of the reaction. Nature, when she needs it for some reason, is capable of several-dozen-order reactions,⁵¹ but in chemistry, a sixth-order reaction is a great rarity. We know of only one example of a reaction having a higher order in the reagent. This is the amination of perylenebiscarboxyimines with azetidine.⁵² It is noteworthy that despite the fundamental difference of this nucleophilic reaction from the electrophilic bromination reactions studied by us, both are outwardly similar in many respects: they proceed without a catalyst under mild conditions only when the reagent serves as a solvent, are first order in the substrate, and their rates are weakly dependent on temperature.

Experimental

The structures and complete assignments of ^1H , ^{13}C , and ^{11}B NMR signals of carboranes **1** and **2** and their derivatives were determined by 2D NMR (^1H - ^1H and ^{11}B - ^{11}B COSY, ^1H - ^{13}C and ^1H - ^{11}B HMQC) on a Bruker Avance-III 600 instrument at 600.30, 150.96, and 192.60 MHz for ^1H , ^{13}C , and ^{11}B , respectively. Chemical shifts were measured for ^1H and ^{13}C relative to residual signals of solvents (CD_2Cl_2 : δ_{H} 5.33 ppm, δ_{C} 53.6 ppm) and for ^{11}B relative to the external standard BF_3OEt_2 (δ_{B} 0 ppm).

Bromine was boiled and distilled over KBr and then over P_2O_5 . CCl_4 was distilled over P_2O_5 , and CD_2Cl_2 was drained by 4 Å molecular sieves. Carboranes **1** and **2** were sublimed in vacuum, and carborane **8** was prepared according to ref. 30.

Preparation of samples: To bromine introduced into an NMR tube, CCl_4 and 0.1 mL of CD_2Cl_2 were carefully added to ensure three distinct layers, and 5–20 mg of solid carborane was then added into the tube. The total volume of the reaction mixture was 0.5 mL. Volumes of Br_2 and CCl_4 were chosen to ensure a desired bromine concentration. The tube was sealed with a PTFE cap and heat shrink tubing. The reaction was launched by stirring the layered content immediately before the recording of NMR spectra. The composition of the reaction mixtures was determined by the integration of ^1H and/or $^{11}\text{B}\{^1\text{H}\}$ NMR spectra.

$^1\text{H}\{^{11}\text{B}\}$, $^{13}\text{C}\{^1\text{H}\}$, and $^{11}\text{B}\{^1\text{H}\}$ NMR spectra with full assignment of the signals of the studied carboranes, except for **4**, are given in SI (p. S4–S40). Carborane **4** was identified by means of spectra from the literature.⁵³ See also refs. 54 (^1H , ^{11}B and ^{13}C of **1**, **3**, **5**), 55 (^{11}B of **1**, **2**, **3**, **5**, **7**), 53 (^1H , ^{11}B and ^{13}C of **1**, **3**, **4**, ^{11}B of **2**, **7**), 32 (^1H and ^{11}B of **8**), and 30 (^1H and ^{11}B of **9**).

NMR spectra of 8,9-dibromo-*o*-carborane **6** (in CD_2Cl_2 , δ , ppm): ^{13}C NMR 51.6 (C1), 46.5 (C2); ^1H NMR 3.79 (H1), 3.83 (H2), 2.76 (H3), 2.50 (H6), 2.22 (H11), 2.65 (H4), 2.55 (H5), 2.59 (H10), 2.79 (H12), 2.57 (H7); ^{11}B NMR –19.57 (B6), –15.67 (B3), –15.55 (B11), –13.94 (B7), –12.86 (B4), –14.10 (B5), –9.29 (B10), –5.52 (B8), –0.77 (B12), 0.30 (B9).

Acknowledgments

The authors gratefully acknowledge the support of the Russian Foundation for Basic Research (grant No. 20-03-00187). The authors would also like to acknowledge the Multi-Access Chemical Research Center SB RAS for spectral and analytical measurements. We thank the Cluster of the Novosibirsk University Scientific Computing Center (<http://www.nusc.ru>) for the computing resources.

ASSOCIATED CONTENT

Supporting Information Available: NMR spectra, kinetics data and quantum chemical calculations.

References

- (1) Shernyukov, A.; Genaev, A.; Salnikov, G.; Rzepa, H.; Shubin, V. Noncatalytic bromination of benzene: A combined computational and experimental study. *J. Comput. Chem.* **2016**, 37, 210–225. DOI: 10.1002/jcc.23985
- (2) Shernyukov, A. V.; Genaev, A. M.; Salnikov, G. E.; Shubin, V. G.; Rzepa, H. S. Elevated reaction order of 1,3,5-tri-tert-butylbenzene bromination as evidence of a clustered polybromide transition state: a combined kinetic and computational study. *Org. Biomol. Chem.*, **2019**, 17, 3781–3789. DOI: 10.1039/C9OB00607A
- (3) (a) Haller, H.; Riedel, S. Recent Discoveries of Polyhalogen Anions – from Bromine to Fluorine. *Z. Anorg. Allg. Chem.* **2014**, 640, 1281–1291. DOI: 10.1002/zaac.201400085. (b) Mann, L.; Senges, G.; Sonnenberg, K.; Haller, H.;

- Riedel, S. Polybromide Dianions and Networks Stabilized by Fluorinated Bromo(triaryl)phosphonium Cations. *Eur. J. Inorg. Chem.* **2018**, 3330–3337. DOI: 10.1002/ejic.201800404. (c) Hasenstab-Riedel, S.; Sonnenberg, K.; Mann, L.; Redeker, F. A.; Schmidt, B. Poly- and Interhalogen Anions from Fluorine to Bromine. *Angew. Chem. Int. Ed.* **2019**, 59(14), 5464–5493. DOI:10.1002/anie.201903197. (d) Haller, H.; Schröder, J.; Riedel, S. Structural Evidence for Undecabromide $[\text{Br}_{11}]^-$. *Angew. Chem. Int. Ed.* **2013**, 52(18), 4937–4940. DOI: 10.1002/anie.201209928
- (4) Poater, J.; Solà, M.; Viñas, C.; Teixidor, F. Hückel's Rule of Aromaticity Categorizes Aromatic closo Boron Hydride Clusters. *Chem. Eur. J.* **2016**, 22, 7437–7443. DOI: 10.1002/chem.201600510
- (5) (a) Hosmane, N. S. (Ed.), *Boron Science New Technologies and Applications*, CRC Press (2011). (b) Hosmane, N. S.; Eagling, R. (Eds.) *Handbook of Boron Science: With Applications in Organometallics, Catalysis, Materials and Medicine*, WORLD SCIENTIFIC (2018)
- (6) Grimes, R. N. *Carboranes* 3rd Ed., Elsevier, Amsterdam and New York (2016)
- (7) Bregadze, V. I. Dicarba-closo-dodecaboranes $\text{C}_2\text{B}_{10}\text{H}_{12}$ and their derivatives. *Chem. Rev.* **1992**, 92, 209–223. DOI:10.1021/cr00010a002
- (8) Mu, X.; Dziedzic, R.; Rheingold, A. L.; Sletten, E.; Axtell, J.; Spokoyny, A. Expanding the Scope of Palladium-Catalyzed B–N Cross-Coupling Chemistry in Carboranes. *ChemRxiv.* **2020**, Preprint. DOI: 10.26434/chemrxiv.12845849.v1
- (9) Bennour, I.; Teixidor, F.; Kelemen Z.; Viñas, C. *m*-Carborane as a Novel Core for Periphery-Decorated Macromolecules. *Molecules* **2020**, 25, 2814. DOI: 10.3390/molecules25122814
- (10) Ol'shevskaya, V. A.; Makarenkov, A. V.; Kononova, E. G.; Peregudov, A. S.; Lyssenko, K. A.; Kalinin, V. N. An efficient synthesis of carboranyl tetrazoles via alkylation of 5-R-1H-tetrazoles with allylcarboranes. *Polyhedron* **2016**, 115, 128–136. DOI:10.1016/j.poly.2016.05.006
- (11) Eriksson, L.; Beletskaya, I.P.; Bregadze, V.I. Sivaev, I, Sjöberg, S. J. Palladium-catalyzed cross-coupling reactions of arylboronic acids and 2-*i*-p-carborane. *Organometallic Chem.* **2002**, 657, 1, 267–272. DOI: 10.1016/S0022-328X(02)01431-6
- (12) Aizawa, K.; Ohta, K.; Endo, Y. Synthesis of 3-aryl-1,2-dicarba-closo-dodecaboranes by Suzuki-Miyaura coupling reaction. *Heterocycles* **2010**, 80, 369–377.
- (13) Xu, T.-T.; Cao, Ke; Zhang, C.-Y.; Wu, Ji; Jiang, L.; Yang, J. Palladium catalyzed selective arylation of o-carboranes via B(4)–H activation: amide induced regioselectivity reversal. *Chem. Commun.* **2018**, 54, 96, 13603–13606. DOI: 10.1039/C8CC08193J
- (14) Eriksson, L.; Winberg, K.J.; Claro, R. T.; Sjöberg, S. Palladium-Catalyzed Heck Reactions of Styrene Derivatives and 2-Iodo-*p*-carborane. *J. Org. Chem.* **2003**, 68, 9, 3569–3573. DOI: 10.1021/jo026248j
- (15) Wi, J.; Cao, K.; Xu, T.T.; Zhang, X.J.; Jiang, L.; Yang, J.; Huang, Y. Palladium catalyzed regioselective mono-alkenylation of o-carboranes via Heck type coupling reaction of a cage B–H bond. *RSC Adv.* **2015**, 5, 91683–91687. DOI: 10.1039/C5RA18555F
- (16) Bangar, P.G.; Jawalkar, P.R.; Dumbre, S.R.; Patil, D.J.; Iyer, S. Silver sequestration of halides for the activation of $\text{Pd}(\text{OAc})_2$ catalyzed Mizoroki-Heck reaction of 1,1 and 1,2 - Disubstituted alkenes. *Appl. Organometal. Chem.* **2018**, 32, 4159–4165. DOI: 10.1002/aoc.4159
- (17) Chaari, M.; Kelemen, Z.; Choquesillo-Lazarte, D.; Gaztelumendi, N.; Teixidor, F.; Viñas, C.; Núñez, R. Efficient blue light emitting materials based on *m*-carborane–anthracene dyads. Structure, photophysics and bioimaging studies. *Biomater. Sci.* **2019**, 7, 5324–5337. DOI:10.1039/c9bm00903e
- (18) Saftić, D.; Studzińska, M.; Paradowska, E.; Piantanida, I.; Baranović, G.; Bialek-Pietras, M.; Leśnikowski, Z. J. Comparative study of the effects of ortho-, meta- and para-carboranes ($\text{C}_2\text{B}_{10}\text{H}_{12}$) on the physicochemical properties, cytotoxicity and antiviral activity of uridine and 2'-deoxyuridine boron cluster conjugates. *Bioorg. Chem.* **2020**, 94, 103466. DOI: 10.1016/j.bioorg.2019.103466
- (19) Kaleta, J.; Akdag, A.; Crespo, R.; Piqueras, M.-C.; Michl, J. Evidence for an Intermediate in the Methylation of $\text{CB}_{11}\text{H}_{12}^-$ with Methyl Triflate: Comparison of Electrophilic Substitution in Cage Boranes and in Arenes. *ChemPlusChem* **2013**, 78, 1174–1183. DOI: 10.1002/cplu.201300219
- (20) Holub, J.; Vishnevskiy, Y. V.; Fanfrlík, J.; Mitzel, N. W.; Tikhonov, D.; Schwabedissen, J.; McKee, M. L.; Hnyk, D. Bromination Mechanism of closo-1,2- $\text{C}_2\text{B}_{10}\text{H}_{12}$ and the Structure of the Resulting 9-Br-closo-1,2- $\text{C}_2\text{B}_{10}\text{H}_{11}$ Determined by Gas Electron Diffraction. *ChemPlusChem* **2020**. DOI:10.1002/cplu.202000543
- (21) Knyazev, S. P.; Gordeev, E. G. Retrieval and analysis of transition states in electrophilic substitution reactions of the carborane(12) series. *Rus. J. General Chem.* **2012**, 82, 1517–1523. DOI: 10.1134/s1070363212090101

- (22) Doborzyński, D. Über die Dielektrizitätskonstante des flüssigen Broms. *Zeitschrift Für Physik* **1930**, 66, 657–668. DOI: 10.1007/bf01421128
- (23) Scilab Enterprises. Scilab: Free and Open Source software for numerical computation (Version 5.5.0), **2012**.
- (24) Zakharkin, L. I.; Kalinin, V. N. On the comparative reactivity of barene and neobarene in electrophilic substitution reactions. *Zh. Obshch. Khim.* **1966**, 36, 2218 (in Russian).
- (25) Taylor, R. Electrophilic Aromatic Substitution; J. Wiley and Sons: New York, **1990**; pp. 25–59.
- (26) Lee, H.; Onak, T.; Jaballas, J.; Tran, U. Deuteration of closo-1,2- and 1,7-C₂B₁₀H₁₂ using C₆D₆/AlCl₃: Mechanistic considerations. *Heteroatom. Chem.* **1998**, 9, 95–102. DOI: 10.1002/(sici)1098-1071(1998)9:1<95::aid-hc12>3.0.co;2-y
- (27) Atkins, P.; Overton, T.; Rourke, J.; Weller, M.; Armstrong, F. Shriver and Atkins' Inorganic Chemistry, 5th Edition; W. H. Freeman, **2009**, p. 135.
- (28) MagicPlot. Lightweight app for data analysis, plotting and nonlinear fitting. <https://magicplot.com/>
- (29) Benson, S. W. The Foundations of Chemical Kinetics, McGraw-Hill Book Company, New York **1960**, p. 82.
- (30) Rudakov, D. A.; Genaev, A. M. Halogenation of carborane alcohol 9-HO-1,2-C₂B₁₀H₁₁, *Rus. Chem. Bull.*, in press
- (31) Semioshkin, A. A.; Sivaev, I. B.; Bregadze, V. I. Cyclic oxonium derivatives of polyhedral boron hydrides and their synthetic applications. *Dalton Trans.* **2008**, 977–992. DOI: 10.1039/b715363e
- (32) Rudakov, D. A.; Genaev, A. M.; Gatilov, Y. V.; Dikuser, E. A.; Zvereva, T. D.; Zubreichuk, Z. P.; Potkin, V. I. Synthesis and structure of 9-hydroxy-1,2-dicarba-closo-dodecaborane(11). *Rus. Chem. Bull.* **2020**, 69, 320–324. DOI: 10.1007/s11172-020-2763-1
- (33) Olah, G. A.; Namanworth, E. Stable Carbonium Ions. XXVIII. Protonated Aliphatic Alcohols. *J. Am. Chem. Soc.* **1966**, 88, 5327–5328. DOI: 10.1021/ja00974a056
- (34) Stanko, V. I.; Brattsev, V. A.; Ovsyannikov, N. N.; Klimova, T. P. Oxidative hydroxylation of *o*-, *m*- and *p*-carboranes(12). *Zh. Obshch. Khim.* **1974**, 44, 2482 [in Russian].
- (35) (a) Laikov, D. N. Fast evaluation of density functional exchange-correlation terms using the expansion of the electron density in auxiliary basis sets. *Chem. Phys. Lett.* **1997**, 281, 151–156. DOI: 10.1016/S0009-2614(97)01206-2
(b) Laikov, D. N.; Ustynyuk, Y. A. PRIRODA-04: a quantum-chemical program suite. New possibilities in the study of molecular systems with the application of parallel computing. *Russ. Chem. Bull.*, **2005**, 54, 820–826.
- (36) Perdew, J. P.; Burke, K.; Ernzerhof, M. Generalized Gradient Approximation Made Simple. *Phys. Rev. Lett.* **1996**, 77, 3865–3868. DOI: 10.1103/PhysRevLett.77.3865
- (37) (a) Laikov, D. N. A New Class of Atomic Basis Functions for Accurate Electronic Structure Calculations of Molecules. *Chem. Phys. Lett.* **2005**, 416, 116–120. DOI: 10.1016/j.cplett.2005.09.046 (b) Laikov, D. N. Atomic basis functions for molecular electronic structure calculations. *Theor. Chem. Acc.* **2019**, 138, 40. DOI: 10.1007/s00214-019-2432-3.
- (38) Chen, X.; Rickard, M. A.; Hull, J. W.; Zheng, C.; Leugers, A.; Simoncic, P. Raman Spectroscopic Investigation of Tetraethylammonium Polybromides *Inorg. Chem.*, **2010**, 49, 8684–8689. DOI: 10.1021/ic100869r
- (39) Genaev, A. M. C₆H₆ + 3Br₂ PES. <http://limor1.nioch.nsc.ru/quant/bromination/>
- (40) (a) Dewar, M. J. S.; Olivella, S.; Rzepa, H. S. Ground states of molecules. 49. MINDO/3 study of the retro-Diels-Alder reaction of cyclohexene. *J. Am. Chem. Soc.* **1978**, 100, 5650–5659. DOI: 10.1021/ja00486a013 (b) Brown, S. B.; Dewar, M. J. S.; Ford, G. P.; Nelson, D. J.; Rzepa, H. S. Ground states of molecules. 51. MNDO (modified neglect of diatomic overlap) calculations of kinetic isotope effects. *J. Am. Chem. Soc.* **1978**, 100, 7832–7836. DOI: 10.1021/ja00493a008 (c) Rzepa, H. S. MNDO SCF-MO calculations of kinetic isotope effects for dehydrochlorination reactions of chloroalkanes. *J. Chem. Soc., Chem. Commun.*, **1981**, 939–940. DOI: 10.1039/C39810000939
- (41) Zhechkov, L.; Heine, T.; Patchkovskii, S.; Seifert, G.; Duarte, H. A. An Efficient a Posteriori Treatment for Dispersion Interaction in Density-Functional-Based Tight Binding. *J. Chem. Theory Comput.* **2005**, 1, 841–847. DOI: 10.1021/ct050065y
- (42) Schmidt, M. W.; Baldridge, K. K.; Boatz, J. A.; Elbert, S. T.; Gordon, M. S.; Jensen, J. H.; Koseki, S.; Matsunaga, N.; Nguyen, K. A.; Su, S. J.; Windus, T. L.; Dupuis, M.; Montgomery, J. A. General atomic and molecular electronic structure system. *J. Comput. Chem.*, **1993**, 14, 1347–1363. DOI: 10.1002/jcc.540141112
- (43) Tomasi, J.; Mennucci, B.; Cammi, R. Quantum Mechanical Continuum Solvation Models. *Chem. Rev.* **2005**, 105, 2999–3093. DOI: 10.1021/cr9904009

- (44) Grimme, S.; Antony, J.; Ehrlich, S.; Krieg, H. A consistent and accurate ab initio parametrization of density functional dispersion correction (DFT-D) for the 94 elements H-Pu. *J. Chem. Phys.* **2010**, 132, 154104/1-19. DOI: 10.1063/1.3382344
- (45) Rzepa, H. S. Computed properties for transition state models for the reaction between bromine and benzene. DOI: 10.14469/ch/191257
- (46) Plešek, J.; Plzák, Z.; Stuchlík, J.; Heřmánek, S. Synthesis of B-alkyl derivatives of o-carborane by alkylation under electrophilic conditions; Scope and limitation. *Collect. Czech. Chem. Commun.* **1981**, 46, 1748–1763. DOI: 10.1135/cccc19811748
- (47) Kraka, E.; Cremer, D. Computational Analysis of the Mechanism of Chemical Reactions in Terms of Reaction Phases: Hidden Intermediates and Hidden Transition States. *Acc. Chem. Res.* **2010**, 43, 591–601. DOI: 10.1021/ar900013p
- (48) Jelinek, T.; Štíbr, B.; Mareš, F.; Plešek, J.; Heřmánek, S. Halogenation of 4,5-dicarba-*arachno*-nonaborane(13), 4,5-C₂B₇H₁₃. *Polyhedron* **1987**, 6(9), 1737–1740. DOI: 10.1016/s0277-5387(00)86544-4
- (49) Douvris, C.; Michl, J. Update 1 of: Chemistry of the Carba-closo-dodecaborate(–) Anion, CB₁₁H₁₂[–]. *Chem. Rev.* **2013**, 113(10), PR179–PR233. DOI: 10.1021/cr400059k
- (50) Frank, R.; Adhikari, A. K.; Auer, H.; Hey-Hawkins, E. Electrophile-Induced Nucleophilic Substitution of the *nido*-Dicarbaundecaborate Anion *nido*-7,8-C₂B₉H₁₂[–] by Conjugated Heterodienes. *Chem. Eur. J.* **2013**, 20(5), 1440–1446. DOI: 10.1002/chem.201303762
- (51) Cao, Z.; Ferrone, F. A. A 50th Order Reaction Predicted and Observed for Sickie Hemoglobin Nucleation. *J. Mol. Biol.*, **1996**, 256, 219–222. DOI: 10.1006/jmbi.1996.0079
- (52) Langhals, H.; Eberspächer, M.; Mayer, P. Uncatalyzed C-H Amination of Aromatic Compounds under Unusually Mild Conditions with Negative Enthalpies of Activation. *Asian J. Org. Chem.* **2017**, 6, 1080–1085. DOI: 10.1002/ajoc.201700106
- (53) Heřmánek, S.; Gregor, V.; Štíbr, B.; Plešek, J.; Janoušek, Z.; Antonovich, V. A. Antipodal and vicinal shift effects in 11B, 13C, and 1H NMR spectra of substituted dicarba-closo-dodecarboranes(12). *Collect. Czech. Chem. Commun.* **1976**, 41, 1492–1499. DOI: 10.1135/cccc19761492
- (54) Štíbr, B.; Tok, O. L.; Holub, J. Quantitative Assessment of Substitution NMR Effects in the Model Series of o-Carborane Derivatives: α-Shift Correlation Method. *Inorg. Chem.* **2017**, 56, 8334–8340. DOI: 10.1021/acs.inorgchem.7b01023
- (55) Siedle, A. R.; Bodner, G. M.; Garber, A. R.; Beer, D. C.; Todd, L. J. Antipodal shielding effects in the boron-11, carbon-13, and phosphorus-31 nuclear magnetic resonance spectra of icosahedral carborane derivatives. *Inorg. Chem.* **1974**, 13, 2321–2324. DOI: 10.1021/ic50140a006

For Table of Contents Only

High experimental kinetic reaction order in bromine, together with quantum chemical modeling, point to a specific mechanism of bromination facilitated by anionic bromine clusters which significantly stabilize the transition state.

